Progress of Theoretical Physics, Vol. 49, No. 3, March 1973

Electronic Structure of Liquid Metals in the Tight-Binding Approximation. I*)

——Single-Site Theory for a Quasi-Orthogonal Set of Atomic Orbitals——

Yoshiaki ISHIDA and Fumiko YONEZAWA

Department of Applied Physics
Tokyo Institute of Technology, Meguroku, Tokyo 152

(Received September 21, 1972)

A tight-binding model is presented to study the density-of-states and some other electronic properties of a liquid metal and an amorphous solid composed of atoms with one-atomic orbital per site. A one-electron Green function is expanded in terms of atomic orbitals and described by a perturbation expansion series in powers of $H'_{mn} \equiv H_{mn} - wS_{mn}$, H_{mn} and S_{mn} being a non-diagonal matrix element of Hamiltonian and an overlap integral, respectively, while w designates the energy. An extended chain approximation is introduced in order to express atomic correlation functions by means of a radial distribution function $g(R_{mn})$. The ensemble-averaged Green function is evaluated based upon the single-site theory of Matsubara and Toyozawa, by which a short-range order of atomic configuration in a liquid metal and an amorphous solid is most properly taken into account. It is mentioned that the present theory is applicable to liquid transition metals and to alkali metals under a supercritical condition. The non-self-consistent treatment in our scheme is shown to be equivalent to the moment-expansion method of Cyrot-Lackmann. In actual implementation of numerical calculation, both the non-self-consistent and self-consistent approximations in our theory are applied and the complete set of atomic orbitals is assumed to be quasi-orthogonal, i.e., $S_{mn} = \delta_{mn}$. As a pair correlation $g(R_{mn})$, we employ three models: (1) A random liquid, (2) a hard-core-random liquid and (3) a hard-core-modified liquid; and one real liquid case; the experimental value of Ni at $T = 1500$°C. The effect of a short-range order in the atomic configuration on the density-of-states, etc., is discussed.

§ 1. Introduction

The purpose of this paper is to propose a method for studying the effect of atomic correlation functions on the density-of-states and some other physical quantities of liquid metals, amorphous solids, doped semiconductors and so on in the modified tight-binding approximation, or alternatively for estimating the behaviour of the microscopic atomic distribution from the observed data of macroscopic electrical properties of structurally-disordered systems.

*) The present work was originally reported at the meeting on "The Properties of Liquid Metals" held in July, 1970, at the Research Institute for Fundamental Physics, Kyoto University and the outline of the theory was introduced in the "Reports on Progress in Lattice Dynamics in Japan" **26** (1970), No. 2.

It is widely accepted that, in liquid metals and in some of amorphous solids, a short-range order in the atomic configuration is preserved in the sense that the coordination number or the concept of nearest-neighbour atoms can be defined, while a long-range order in the distribution of atoms is destroyed. It is expected that the effect of local ordering in the atomic configuration becomes more distinguished in the systems for which the nearly-free-electron approximation fails to work. There has been no systematic and self-consistent theory established on the tight-binding basis so as to take properly into account the characteristic feature of the atomic configuration in systems having structural disorder, although some attempts have been suggested in the framework of non-self-consistent theories.[1),2)] Even in the substitutionally disordered alloys or cellular-disordered systems in which the regularity in the array of atoms makes the problem easier, the best single-site theory—the coherent potential approximation—has been successful in principle only for such site-random systems that the distribution function $\mathcal{P}(\{\varepsilon_n\})$ of site-random variables $\{\varepsilon_n\}$ is assumed to be statistically independent, i.e., the function is described as $\mathcal{P}(\{\varepsilon_n\})=\prod_n P(\varepsilon_n)$. The present theory is, therefore, the first that assures the self-consistent treatment in the tight-binding model and gives due consideration to the effect of the local ordering in the distribution of atoms and the effect of clustering as well.

As in the ordinary tight-binding approach, let us assume that the wave function can be expanded in terms of one-atomic orbital per site. Note that the dynamical effect of atoms is eliminated from the present theory, since the time-dependent behaviour of the atomic configuration is not essential so far as we are concerned with the physical properties of electrons whose mass is far smaller than that of atoms. In an independent electron model, the one-electron Green function is expanded in the non-degenerate atomic orbitals, and is described in a locator-propagator-type perturbation expansion series. What we need in discussing the macroscopic feature of the single-electron properties of the system is the effective Green function ensemble-averaged over all possible configurations of atoms. In the process of averaging the terms in the perturbation series of the Green function, atomic correlation functions $\rho^n g^{(n)}(\boldsymbol{R}_1, \boldsymbol{R}_2, \cdots, \boldsymbol{R}_n)$ explicitly enter into the formulation. A complete knowledge of $g^{(n)}(\boldsymbol{R}_1, \boldsymbol{R}_2, \cdots, \boldsymbol{R}_n)$ for all n is not attained either from the theoretical base nor from the experimental results, for one thing, and even if n-body correlation functions are given, it is substantially impossible, for another thing, to construct a theory which takes a full account of the higher atomic correlation functions. Usually, $g^{(n)}(\boldsymbol{R}_1, \boldsymbol{R}_2, \cdots, \boldsymbol{R}_n)$ is approximated by some appropriate functional of lower-order correlation functions $g^{(m)}(\boldsymbol{R}_1, \boldsymbol{R}_2, \cdots, \boldsymbol{R}_n)$ with $m<n$, and for that purpose we introduce in this paper an extended chain approximation which is convenient for the self-consistent treatment of the ensemble-averaged terms.

In order to derive a reasonably approximate expression for the ensemble-averaged Green function, we modify the single-site theory of Matsubara and

Toyozawa (MT theory)[3] which has originally been proposed to study the density-of-states and conductivity of an impurity band in a doped semiconductor. The MT method proves to be advantageous to describe the clustering effect when a short-range order in the distribution of atoms is important. The theory developed in the present article is compared with the approximation by Schwartz and Ehrenreich[4] in this context. It is shown that the non-self-consistent counterpart of our theory compares with the quasi-crystalline approximation of Lax[5] and corresponds to the moment-expansion method of Cyrot-Lackmann.[1]

In the actual calculation of the density-of-states and other electrical properties, the extended chain approximation is applied so that the atomic correlation functions $g^{(n)}(\boldsymbol{R}_1, \boldsymbol{R}_2, \cdots, \boldsymbol{R}_n)$ is described only by means of $g^{(2)}(R)$, and several model- and real-pair correlation functions are employed. As a nondegenerate atomic orbital, we use the $1s$ wave function of an isolated atom defined by the effective Bohr radius a^* characterizing the atom under consideration. Although our theory is available to a non-orthogonal set of atomic states, we assume in the present paper that the set of atomic wave functions is quasi-orthogonal; the overlap integral S_{mn} is taken to be δ_{mn}. Since consideration of non-orthogonality is expected to guarantee the validity of the tight-binding approximation for somewhat extended wave functions,[6] the results based upon a non-orthogonal set of atomic orbitals will be presented in a succeeding paper.[7]

The present theory is in principle applicable to a structurally disordered system in which the tight-binding representation of the electronic wave function is appropriate and the effect of a short-range order is eminent. Some sorts of liquid metals, amorphous solids and probably doped semiconductors are the candidates. Especially, we can consider two special examples:

1) The first example is liquid transition metals. Since the tight-binding approximation has achieved some success in illustrating the narrow d band of solid transition metals, it appears meaningful to study, in the same scheme, the feature of such a band in a liquid state. Though the assumptions of one atomic state per site and of the isotropic atomic orbital may oversimplify the situation, the characteristic behaviour of these systems will be clarified.

2) Another example is alkali metals under high temperature and high pressure, in which the average interatomic distance is increased too much in order for an approach based upon the free-electron model to be available. When the interatomic distance is moderately large in alkali metals, the conduction takes place via electron transfer between localized atomic orbitals and hence the tight-binding approximation becomes appropriate. The problem concerned with alkali metals of low density is interesting in relation with the recent experimental results on the electronic properties of these systems under supercritical condition.[8] Although the Coulomb interaction between electrons may play an important role in such metals, we confine ourselves to an independent electron picture in the present article and the special problem of supercritical fluid will be reported in

a separate paper where the correlation effect of electrons is taken into account.[9]

The formulation of the problem is given in § 2, where the extended chain approximation is introduced and the single-site theory is developed. The non-self-consistent (NSC) method and the results of numerical calculation by means of the NSC technique are presented in § 3, while the self-consistent (SC) approach is explained in § 4. In the following section, § 5, the density-of-states in the SC theory is evaluated by making use of several models and experimental data for $g^{(2)}(R)$ and the effect of a short-range order is illustrated. Some remarks on the localization of electrons and conductivity are made in § 6 and discussion is given in § 7.

§ 2. Single-site theory with extended chain approximation

By means of the Hamiltonian operator H for a given configuration of atoms, the one-electron Green function $G(\boldsymbol{r}, \boldsymbol{r}')$ is defined by

$$(E-H)G(\boldsymbol{r}, \boldsymbol{r}') = \delta(\boldsymbol{r}-\boldsymbol{r}'). \tag{2·1}$$

According to the formulation of Roth,[2] let us expand $G(\boldsymbol{r}, \boldsymbol{r}')$ in terms of atomic orbitals $\varphi_m(\boldsymbol{r}) = \varphi(\boldsymbol{r}-\boldsymbol{R}_m)$:

$$G(\boldsymbol{r}, \boldsymbol{r}') = \sum_{mn} \varphi_m(\boldsymbol{r}) G_{mn} \varphi_n(\boldsymbol{r}'). \tag{2·2}$$

From Eqs. (2·1) and (2·2), the equation for G_{mn} is obtained in the form

$$\sum_l (ES_{ml} - H_{ml}) G_{ln} = \delta_{mn}, \tag{2·3}$$

where S_{mn} and H_{mn} are respectively overlap and Hamiltonian matrices given by

$$S_{mn} = \langle m|n\rangle, \tag{2·4}$$

$$H_{mn} = \langle m|H|n\rangle. \tag{2·5}$$

Since the overlap integral S_{mn} is not generally equal to δ_{mn}, it is convenient to rearrange Eq. (2·3) by writing $H'_{mn} = H_{mn} - ES_{mn}$ for $m \neq n$; thus we have

$$\sum_l (E\delta_{ml} - H'_{ml}) G_{ln} = \delta_{mn}. \tag{2·6}$$

The matrix element of the Green function is therefore expanded in powers of H'_{mn} in a locator-interactor perturbation series:

$$G_{mn} = G_m^{(0)}\delta_{mn} + G_m^{(0)}(1-\delta_{mn}) H'_{mn} G_n^{(0)} + \sum_{l(\neq m, n)} G_m^{(0)} H'_{ml} G_l^{(0)} H'_{ln} G_n^{(0)} + \cdots, \tag{2·7}$$

in which $G_n^{(0)}$ is an unperturbed locator at $\boldsymbol{R}_n$ determined by $G_n^{(0)} = [E - H_{nn}]^{-1}$.

For the purpose of introducing some simplifying assumptions, let us assume, for example, the one-electron Hamiltonian of an electron interacting with N atoms by a set of additive atomic potential $V(\boldsymbol{r}-\boldsymbol{R}_m) = V_m$.

$$H = T + \sum_m V(\boldsymbol{r}-\boldsymbol{R}_m) = T + \sum_m V_m. \tag{2·8}$$

Assumptions employed in the present paper are as follows:

(1) Two-centre integrals of the type of $\langle n|V_m|n\rangle$ are neglected with respect to two-ecntre integrals of the type of $\langle n|V_m|m\rangle$. This assumption leads to the result that $G_n^{(0)}=G^{(0)}$ is a constant, independent of site n and the distribution of the other atoms.

(2) Three-centre integrals of the type of $\langle n|V_l|m\rangle$ are regarded as small compared with two-centre integrals of the type of $\langle n|V_n|m\rangle$ and discarded. This concludes that H'_{mn} for $m=n$ is a function only of the relative positions $\boldsymbol{R}_{mn}=\boldsymbol{R}_n-\boldsymbol{R}_m$; i.e., $H'_{mn}=H'(\boldsymbol{R}_{mn})$.

(3) The atomic functions centred on different atoms m and n are considered to be orthogonal, i.e., $\langle m|n\rangle$ is neglected with respect to $\langle n|n\rangle=1$. Thus we have $H'_{mn}=H_{mn}=H(\boldsymbol{R}_{mn})$. As a result, Eq. (2·7) is now rewritten as

$$G_{mn}=G^{(0)}\delta_{mn}+[G^{(0)}]^2(1-\delta_{mn})H(\boldsymbol{R}_{mn})+[G^{(0)}]^3\sum_{l(\neq m,n)}H(\boldsymbol{R}_{ml})H(\boldsymbol{R}_{ln})$$
$$+[G^{(0)}]^4\sum_{(m\neq)l\neq h(\neq n)}H(\boldsymbol{R}_{ml})H(\boldsymbol{R}_{lh})H(\boldsymbol{R}_{hn})+\cdots. \qquad (2\cdot9)$$

The mean density-of-states $n(E)$ is calculated by averaging $T_r\delta(E-H)$ over all possible distributions of atoms and thus related to the one-electron Green function as

$$n(E)=\langle \mathrm{Tr}\,\delta(E-H)\rangle=\frac{-1}{\pi}\,\mathrm{Im}\sum_m\langle G_{mm}(E^+)\rangle=\frac{-N}{\pi}\,\mathrm{Im}\,\langle G_{mm}\rangle. \qquad (2\cdot10)$$

The ensemble average denoted by angular brackets is defined by

$$\langle\mathcal{F}(\{\boldsymbol{R}_n\})\rangle=\int\mathcal{F}(\{\boldsymbol{R}_n\})\rho^N g^{(N)}(\boldsymbol{R}_1,\cdots,\boldsymbol{R}_N)\,d\boldsymbol{R}_1 d\boldsymbol{R}_2\cdots d\boldsymbol{R}_N, \qquad (2\cdot11)$$

where $\mathcal{F}(\{\boldsymbol{R}_n\})\equiv\mathcal{F}(\boldsymbol{R}_1,\cdots,\boldsymbol{R}_N)$ is an arbitrary function of $\boldsymbol{R}_1,\boldsymbol{R}_2,\cdots,\boldsymbol{R}_N$; ρ the number density of atoms, given by $\rho=N/\Omega$ for the number N of atoms and the volume Ω of the system; and $\rho^n g^{(n)}(\boldsymbol{R}_1,\cdots,\boldsymbol{R}_n)$ for $n=1,2,3,\cdots,N$ is the atomic correlation function which determines the probability of finding a set of n atoms located at $\boldsymbol{R}_1,\boldsymbol{R}_2,\cdots,\boldsymbol{R}_n$. In the problem of liquid metals, the n-body correlation function is usually given by

$$\rho^n g^{(n)}(\boldsymbol{R}_1,\boldsymbol{R}_2,\cdots,\boldsymbol{R}_n)=\frac{N!}{(N-n)!}\,\frac{\int\exp[-\beta U(\boldsymbol{R}_1,\boldsymbol{R}_2,\cdots,\boldsymbol{R}_N)]\,d\boldsymbol{R}_{n+1}\cdots d\boldsymbol{R}_N}{\int\exp[-\beta U(\boldsymbol{R}_1,\boldsymbol{R}_2,\cdots,\boldsymbol{R}_N)]\,d\boldsymbol{R}_1 d\boldsymbol{R}_2\cdots d\boldsymbol{R}_N}, \qquad (2\cdot12)$$

where $\beta=1/kT$ and $U(\boldsymbol{R}_1,\boldsymbol{R}_2,\cdots,\boldsymbol{R}_N)$ is the energy of a given configuration $\{\boldsymbol{R}_n\}$.

Returning to Eq. (2·9) of our problem, we find that sums are defined to run over a set of discrete variables where any two of successive variables are different from each other. For illustration, let us consider for example the fourth-order term $H(\boldsymbol{R}_{ml})H(\boldsymbol{R}_{lh})H(\boldsymbol{R}_{hk})H(\boldsymbol{R}_{km})$ in which only the term $m=n$ of interest in the calculation of $n(E)$ in Eq. (2·10) is accounted. The restriction over the

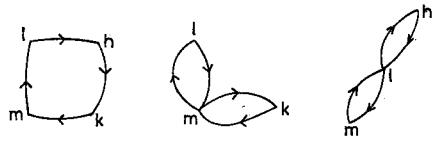

Fig. 1. Three distinct cases for the summation variables in the fourth-order term $H(\boldsymbol{R}_{ml})H(\boldsymbol{R}_{lh})H(\boldsymbol{R}_{hk})H(\boldsymbol{R}_{km})$. (1) all the four variables are different from one another: (2) $\boldsymbol{R}_h=\boldsymbol{R}_m$ and (3) $\boldsymbol{R}_l=\boldsymbol{R}_k$.

summation is such that $\boldsymbol{R}_m \neq \boldsymbol{R}_l$, $\boldsymbol{R}_l \neq \boldsymbol{R}_h$, $\boldsymbol{R}_h \neq \boldsymbol{R}_k$ and $\boldsymbol{R}_k \neq \boldsymbol{R}_m$. It must be noted, however, that, still then, four distinct cases are possible; that is to say, (a) the case where all the four points $\boldsymbol{R}_l$, $\boldsymbol{R}_h$, $\boldsymbol{R}_k$ and $\boldsymbol{R}_m$ are different from one another, (b) the case in which $\boldsymbol{R}_h$ is identical with $\boldsymbol{R}_m$, (c) the case in which $\boldsymbol{R}_l$ is identical with $\boldsymbol{R}_k$, and (d) the case $\boldsymbol{R}_m=\boldsymbol{R}_h$ and $\boldsymbol{R}_l=\boldsymbol{R}_k$. Explanation of the situation is facilitated by the diagrammatic expression as Figs. 1 (a) to 1 (c). (The case (d) is not shown in the figure, because this is not a single-site term.) For carrying out the average, these three terms shown in Fig. 1 should be treated individually. Namely, for case (a), the average process is effected by the replacement

$$\sum_{\text{case (a)}} H(\boldsymbol{R}_{ml})H(\boldsymbol{R}_{lh})H(\boldsymbol{R}_{hk})H(\boldsymbol{R}_{km})$$

$$\to \rho^4 \int H(\boldsymbol{R}_{ml})H(\boldsymbol{R}_{lh})H(\boldsymbol{R}_{hk})H(\boldsymbol{R}_{km})\, g^{(4)}(\boldsymbol{R}_m, \boldsymbol{R}_l, \boldsymbol{R}_h, \boldsymbol{R}_k)\, d\boldsymbol{R}_l d\boldsymbol{R}_h d\boldsymbol{R}_k\,, \tag{2·13}$$

while for cases (b) and (c), the configuration averages are concerned with three-body atomic distribution function as

$$\sum_{\text{case (b)}} H(\boldsymbol{R}_{ml})H(\boldsymbol{R}_{lm})H(\boldsymbol{R}_{mk})H(\boldsymbol{R}_{km})$$

$$\to \rho^3 \int H(\boldsymbol{R}_{ml})H(\boldsymbol{R}_{lm})H(\boldsymbol{R}_{mk})H(\boldsymbol{R}_{km})\, g^{(3)}(\boldsymbol{R}_m, \boldsymbol{R}_l, \boldsymbol{R}_k)\, d\boldsymbol{R}_l d\boldsymbol{R}_k \tag{2·14}$$

and

$$\sum_{\text{case (c)}} H(\boldsymbol{R}_{ml})H(\boldsymbol{R}_{lh})H(\boldsymbol{R}_{hl})H(\boldsymbol{R}_{lm})$$

$$\to \rho^3 \int H(\boldsymbol{R}_{ml})H(\boldsymbol{R}_{lh})H(\boldsymbol{R}_{hl})H(\boldsymbol{R}_{lm})\, g^{(3)}(\boldsymbol{R}_m, \boldsymbol{R}_l, \boldsymbol{R}_h)\, d\boldsymbol{R}_l d\boldsymbol{R}_h\,. \tag{2·15}$$

The completely analogous situation is met for all the higher-order terms and there again the diagrams prove to serve as a great help. For better understanding, take the νth-order term, for instance, as shown in Fig. 2 in which the consideration is confined to single-site diagrams alone. The term with all ν distinct variables (Fig. 2(a)) is averaged by means of the ν-body correlation function $g^{(\nu)}(\boldsymbol{R}_m, \boldsymbol{R}_1, \cdots, \boldsymbol{R}_{\nu-1})$, while the diagram with μ irreducible parts connected at articulation points is related to $g^{(\nu-\mu+1)}(\boldsymbol{R}_m, \boldsymbol{R}_1, \cdots, \boldsymbol{R}_{\nu-\mu})$. Note that there are

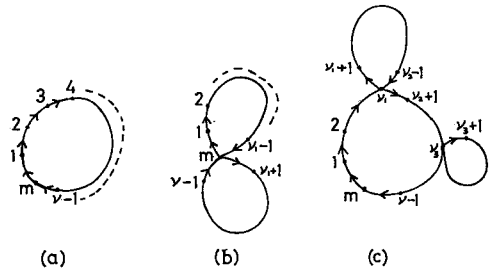

Fig. 2. A general example of νth-order term. Some of possible cases are illustrated; (a) all variables are distinct, (b) one of the intermediate variables is identical with the original site $\boldsymbol{R}_m$ and (c) $\boldsymbol{R}_{\nu_1}=\boldsymbol{R}_{\nu_2}$ and $\boldsymbol{R}_{\nu_3}=\boldsymbol{R}_{\nu_4}$ for $\nu_1<\nu_2<\nu_3<\nu_4$.

two irreducible parts for Fig. 2(b) and three for Fig. 2(c).

Now, the next step is to approximate the many-body correlation functions $g^{(n)}(\boldsymbol{R}_1, \boldsymbol{R}_2, \cdots, \boldsymbol{R}_n)$ of atomic distribution.

Let us first pick up the simplest diagrams as Figs. 1(a) and 2(a) where all the variables are distinct. For these terms, we employ a chain product of pair-correlation functions[1] determined as

$$g^{(n)}(\boldsymbol{R}_1, \boldsymbol{R}_2, \cdots, \boldsymbol{R}_n)=g^{(2)}(\boldsymbol{R}_{12})\,g^{(2)}(\boldsymbol{R}_{23})\cdots g^{(2)}(\boldsymbol{R}_{n-1,n})\,g^{(2)}(\boldsymbol{R}_{n,1}). \tag{2·16}$$

With this type of chain approximation, Eq. (2·13) is easily converted to a factorized form as follows:

$$\begin{aligned}
&\rho^4\int H(\boldsymbol{R}_{ml})H(\boldsymbol{R}_{lh})H(\boldsymbol{R}_{hk})H(\boldsymbol{R}_{km})\,g^{(4)}(\boldsymbol{R}_m, \boldsymbol{R}_l, \boldsymbol{R}_h, \boldsymbol{R}_k)\,d\boldsymbol{R}_l d\boldsymbol{R}_h d\boldsymbol{R}_k\\
&\quad=\rho^4\int H(\boldsymbol{R}_{ml})H(\boldsymbol{R}_{lh})H(\boldsymbol{R}_{hk})H(\boldsymbol{R}_{kn})\,g^{(2)}(\boldsymbol{R}_{ml})\,g^{(2)}(\boldsymbol{R}_{lh})\,g^{(2)}(\boldsymbol{R}_{hk})\,g^{(2)}(\boldsymbol{R}_{kn})\\
&\qquad\times\exp[i\boldsymbol{k}\cdot(\boldsymbol{R}_{ml}+\boldsymbol{R}_{lh}+\boldsymbol{R}_{hk}+\boldsymbol{R}_{kn})]\frac{d\boldsymbol{k}}{(2\pi)^3}d\boldsymbol{R}_{ml}d\boldsymbol{R}_{lh}d\boldsymbol{R}_{hk}d\boldsymbol{R}_{kn}\\
&\quad=\int[\rho V(\boldsymbol{k})]^4\frac{d\boldsymbol{k}}{(2\pi)^3},
\end{aligned} \tag{2·17}$$

where

$$V(\boldsymbol{k})=\int H(\boldsymbol{R})\,g^{(2)}(\boldsymbol{R})\exp[i\boldsymbol{k}\cdot\boldsymbol{R}]\,d\boldsymbol{R}, \tag{2·18}$$

and generally the contribution from the νth-order term as shown in Fig. 2(a) becomes $\int[\rho V(\boldsymbol{k})]^\nu d\boldsymbol{k}/(2\pi)^3$. For such diagrams with articulation points as shown in Figs. 2(b) and 2(c), we extend the concept of the chain approximation so that (1) we can assume the correlation function described by a product of the lower-order correlation functions denoting the respective irreducible parts; for instance,

$$g^{(\nu-1)}(\boldsymbol{R}_m, \boldsymbol{R}_1, \boldsymbol{R}_2, \cdots, \boldsymbol{R}_{\nu-1})=g^{(\nu_1)}(\boldsymbol{R}_m, \boldsymbol{R}_1, \cdots, \boldsymbol{R}_{\nu_1-1})\,g^{(\nu-\nu_1)}(\boldsymbol{R}_m, \boldsymbol{R}_{\nu_1+1}, \boldsymbol{R}_{\nu_1+2}, \cdots, \boldsymbol{R}_{\nu-1}) \tag{2·19}$$

for Fig. 2(b), and that (2) we apply the chain approximation to each irreducible correlation functions. Thus, we have for Fig. 2(b)

$$g^{(2)}(\boldsymbol{R}_{m1})g^{(2)}(\boldsymbol{R}_{12})\cdots g^{(2)}(\boldsymbol{R}_{\nu_1-1,m})g^{(2)}(\boldsymbol{R}_{m,\nu_1+1})g^{(2)}(\boldsymbol{R}_{\nu_1+1,\nu_1+2})\cdots g^{(2)}(\boldsymbol{R}_{\nu-1,m}), \quad (2\cdot20)$$

and the averaged result is written as

$$\rho^{\nu-1}\int[V(\boldsymbol{k}_1)]^{\nu_1}\frac{d\boldsymbol{k}_1}{(2\pi)^3}\int[V(\boldsymbol{k}_2)]^{\nu-\nu_1}\frac{d\boldsymbol{k}_2}{(2\pi)^3}. \quad (2\cdot21)$$

Although the site $\boldsymbol{R}_m$ corresponding to the articulation point appears in both sub-functions as seen from Eqs. (2·19) and (2·20), it is readily shown that the asumption of spatial homogeneity removes any complexity and the ensemble-average is expressed in a factorized form as Eq. (2·21).

With the aid of the extended chain approximation, our formulation becomes substantially parallel to that of the tight-binding model for a completely random distribution of atoms where $g^{(n)}(\boldsymbol{R}_1,\cdots,\boldsymbol{R}_n)=1$ for all n and for any set of $\{\boldsymbol{R}\}$. The interpretation is achieved by the replacement as shown in Fig. 3(b) where the dotted line represents the pair correlation function $g^{(2)}(\boldsymbol{R}_{mn})$ (Fig. 3(a)) and the arrowed solid line designates the mn elements of the Hamiltonian matrix. The only exception is the diagrams of the type as Fig. 3(c) for which one dotted line is assigned to two solid lines. It must be emphasized here again that only the single-site diagrams are taken into account throughout the present section, where single-site diagrams are those diagrams in which any two rings formed of solid-dotted lines corresponding to $H(\boldsymbol{R}_{mn})g(\boldsymbol{R}_{mn})$ are connected with each other by a single common site (called an articulation point). The many-site diagrams as shown in Fig. 17 will be discussed in § 7.

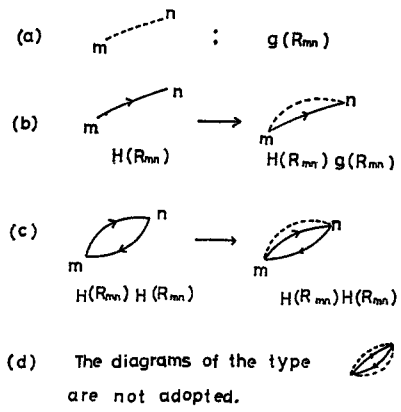

Fig. 3. The prescription to interpret the tight-binding formulation for a completely random distribution of atoms into the case with the extended chain approximation for the atomic correlation functions.

§ 3. Non-self-consistent theory

In the present section, we study the simplest solution for the averaged Green function $\langle G_{mm}\rangle$ along the line of the last section. Let us consider only the self-avoiding paths as given by Figs. 1(a) and 2(a) where none of the sites are identical among themselves. In this case, the ordinary chain approximation is enough to give the factorized expression for each term in the perturbation expansion and hence we have a geometric series of the form

$$\langle G_{mm}\rangle = G^{(0)} + [G^{(0)}]^2\rho\int H(\boldsymbol{R})H(-\boldsymbol{R})g(\boldsymbol{R})d\boldsymbol{R} + \sum_{\nu=3}^{\infty}[G^{(0)}]^{\nu+1}\rho^{\nu}\int[V(\boldsymbol{k})]^{\nu}\frac{d\boldsymbol{k}}{(2\pi)^3}$$
$$= \int\frac{1}{[G^{(0)}]^{-1}-\rho V(\boldsymbol{k})}\frac{d\boldsymbol{k}}{(2\pi)^3} + [G^{(0)}]^2\int\rho V(\boldsymbol{k})[V_0(\boldsymbol{k})-\rho V(\boldsymbol{k})]\frac{d\boldsymbol{k}}{(2\pi)^3}, \tag{3·1}$$

where use is made of $V_0(\boldsymbol{k})=\int H(\boldsymbol{R})\exp[i\boldsymbol{k}\cdot\boldsymbol{R}]d\boldsymbol{R}$ and of the relation

$$\int V(\boldsymbol{k})\frac{d\boldsymbol{k}}{(2\pi)^3} = H(\boldsymbol{R}=0)g^{(2)}(\boldsymbol{R}=0)=0\,. \tag{3·2}$$

There the density-of-states is given by

$$n(E) = \int\delta(E-\rho V(\boldsymbol{k}))\frac{d\boldsymbol{k}}{(2\pi)^3}, \tag{3·3}$$

in which the zero of energy is so defined that $H_{nn}=0$. This is equivalent to the result obtained from the moment-expansion method of Cyrot-Lackmann.[1] It must be noted that the formulation employed by Roth[2] according to the quasi-crystalline approximation of Lax[5] differs from ours in that the diagram in Fig. 3(d) instead of Fig. 3(c) is included in the theory of Roth, which is shown to lead to an unphysical result.[7] When the atomic orbital is chosen to be isotropic, $H(\boldsymbol{R})$ is a function of $R=|\boldsymbol{R}|$. On the other hand, the pair correlation function is described as $g^{(2)}(R)=g(R)$ with $g(R)$ expressing the radial distribution function. Thus, $V(\boldsymbol{k})$ is shown to be a function of $k=|\boldsymbol{k}|$ alone, which reduces Eq. (3·3) to a simpler form

$$n(E) = \frac{1}{2\pi^2}\sum_s\frac{k_s^2}{\rho|\partial V_k/\partial k|_{k=k_s}} \tag{3·4}$$

where k_s is the s-th solution of $E-\rho V_k=0$.

For the actual development of numerical calculation we adopt the atomic wave function of 1s-like orbital defined by

$$\varphi_m(\boldsymbol{r}) \equiv \varphi(\boldsymbol{r}-\boldsymbol{R}_m) = (1/\pi a^{*3})^{1/2}\exp[-|\boldsymbol{r}-\boldsymbol{R}_m|/a^*], \tag{3·5}$$

where a^* is the effective Bohr radius. When the potential $V(\boldsymbol{r}-\boldsymbol{R}_m)$ in Eq. (2·8) is given by the Coulomb interaction between an electron at $\boldsymbol{r}$ and an ion at $\boldsymbol{R}_m$, i.e., $V(\boldsymbol{r}-\boldsymbol{R}_m)=-Ze^2/\kappa|\boldsymbol{r}-\boldsymbol{R}_m|$, then the off-diagonal matrix element of H is written as

$$H_{mn} \equiv H(\boldsymbol{R}_{mn}) = -V_0(1+R_{mn}/a^*)\exp[-R_{mn}/a^*]. \tag{3·6}$$

The energy unit is taken to be $V_0=Ze^2/\kappa a^*$, Z being the charge of ion and κ the dielectric constant. Besides energy, it is convenient to use dimensionless variables and for that purpose the unit of distance, momentum, concentration,

the Fourier-transformed energy and the density-of-states are chosen as follows: $\boldsymbol{R}/a^*=\boldsymbol{r}$, $\boldsymbol{k}a^*=\boldsymbol{t}$, $32\pi\rho a^{*3}=p$, $V(k)/V_0a^{*3}=v(t)$ and $n(E)V_0a^{*3}=n(w)$. Then Eq. (3·4) is rewritten as

$$n(w)=\frac{16}{\pi}\sum_s \frac{t_s^2}{p|\partial v(t)/\partial t|_{t=t_s}}, \tag{3·4′}$$

where t_s is the s-th solution of $w-pv(t)/32\pi=0$.

In the present section, we apply Eq. (3·4) to a random liquid and a hard-core-random liquid.

3.1 *Random liquid*

Let us first consider a random liquid for which $g(R)=1$ for all R and then we have $v(t)=-32\pi/(1+t^2)^3$, which is shown by a dotted line in Fig. 4. The density-of-states $n(w)$ is evaluated on the basis of Eq. (3·4) and depicted by a dotted line in Fig. 5. Note that $w=E/V_0$.

3.2 *Hard-core-random liquid*

A more realistic but rather simple model of a liquid metal is a hard-core-random liquid for which

$$g(R)=\begin{cases}0, & R/a^*<\sigma,\\ 1, & R/a^*\geq\sigma,\end{cases} \tag{3·7}$$

where σa^* is called a hard-core diameter. The packing fraction η is related to σ and p by

$$\eta=\rho\frac{4\pi}{3}\left(\frac{\sigma a^*}{2}\right)^3=\frac{p\sigma^3}{192}. \tag{3·8}$$

The case of a random liquid discussed in subsection 3.1 is regarded as a limit of $\sigma=0$ or $\eta=0$. Equation (2·18) is calculated as

$$v(t)=-\frac{4\pi}{t}\frac{e^{-\sigma}}{(1+t^2)^3}[\{8+(1+t^2)(5+t^2)\sigma+(1+t^2)^2\sigma^2\}t\cos\sigma t + \{-(t^4+6t^2-3)-(t^2+1)(t^2-3)\sigma+(t^2+1)^2\sigma^2\}\sin\sigma t]. \tag{3·9}$$

The curves $v(t)$ vs. t with $p=0.2$ are shown in Fig. 4 for several values of η (or equivalently σ). It is apparent that the oscillatory property of $\sin(\sigma t)$ and $\cos(\sigma t)$ in Eq. (3·9) causes an infinite sequence of extrema in these curves for $\eta\neq 0$. On the other hand, we can easily see from Eq. (3·4) that the existence of extrema in $v(t)$ results in an infinite sequence of singularities in the density-of-states. This sort of difficulty is not encountered in the problem of regular systems because in this case the integral of Eq. (3·3) is restricted within the first Brillouin zone, while no such region of integration variables is defined in disordered systems. Although non-orthogonality of atomic orbitals introduces a

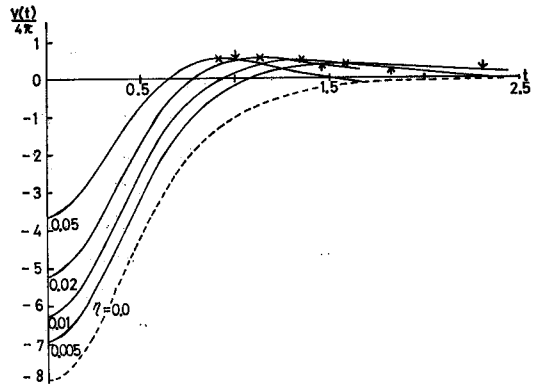

Fig. 4. The dispersion relation curve $v(t)/4\pi$ vs. t. The dotted line corresponds to the case $\eta=0.0$, while the four solid lines represents $v(t)$ for $\eta=0.005$, 0.01, 0.02 and 0.05 respectively. Arrows designate t_η, while crosses t_0. The concentration p is fixed to be 0.2.

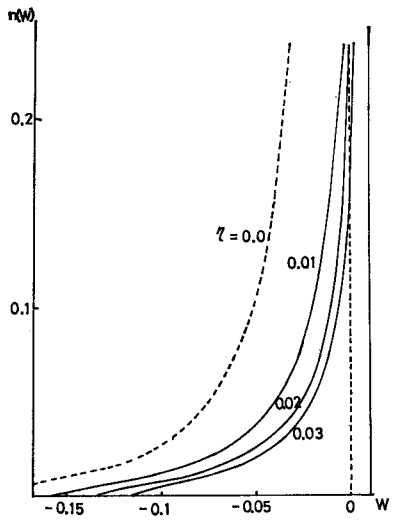

Fig. 5. The density-of-states for $p=0.2$ and for $\eta=0.0$ (the dotted line), 0.01, 0.02, 0.03 (solid lines).

natural cutoff for the integral,[2] the situation is not completely improved. One possible cutoff may be determined from the relation $(2\pi/\sigma)^3=(4\pi/3)k_\eta^3$, where the volume of the first quasi-Brillouin zone for a simple cubic lattice is connected to σ and equated to a sphere with radius k_η. The cutoff momenta $t_\eta=k_\eta a^*$ are denoted by arrows in Fig. 4, while the first maxima t_0 are indicated by crosses. For reasonable values of η, the cutoff covers only the first maximum and approaches infinity with $\eta\to 0$ (see Fig. 6). The band-edges obtained with $t_\eta \geq t_0$ are illustrated in Fig. 7.

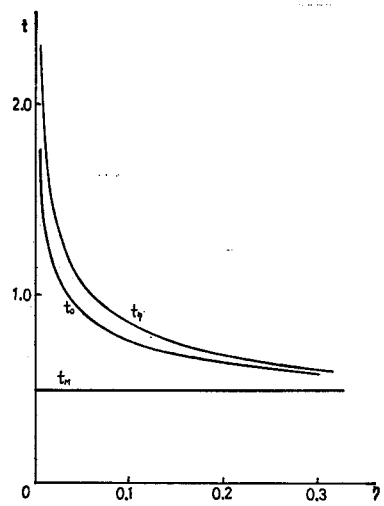

Fig. 6. The cutoff t_η and the value of $t=t_0$ at the first maximum of $v(t)$ represented as functions of η. The cutoff t_M is also denoted.

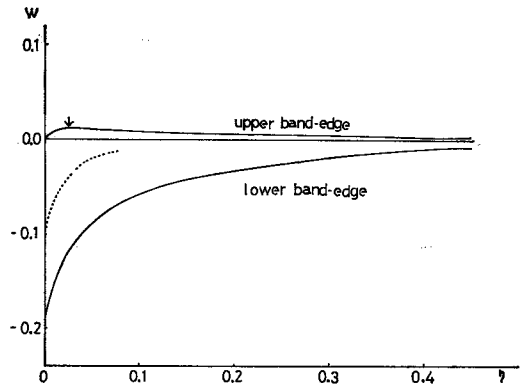

Fig. 7. The upper and lower band-edges vs. η, which are determined from the cutoff t_η. The dotted line shows the upper band-edge yielded from the cutoff $k_M=t_M a^*$.

The dotted line represents an upper band-edge determined from the cutoff $t_M = k_M a^*$ estimated by $(2\pi/d)^3 = (4\pi/3)k_M^3$, d the lattice constant satisfying $Nd^3 = 1$.[1] Unphysical behaviour of the band-edge suggests that this way of determining k_M is not appropriate. The density-of-states calculated with the cutoff k_η is expressed by a respective solid line in Fig. 5. Unsatisfactory features of the non-self-consistent theory are: (1) The density-of-states has a singularity at the upper band-edge and may have more, even if the natural cutoff is introduced, (2) for $\eta=0$ (a random liquid), non-zero value of $n(w)$ is obtained only for $w<0$ and (3) the η-dependence of the upper band-edge is not physically explained. It is expected that these demerits are eliminated when a self-consistent formulation is applied, which is discussed in the succeeding two sections.

§ 4. Self-consistent theory

According to the definition of single-site diagrams (see the last paragraph of § 2), the diagrams in Figs. 1 and 2 are all included in the category of single-site diagrams. As has been explained in § 2, the extended chain approximation enables us to write the contributions from these single-site terms in factorized forms like Eq. (2·21). When this is the case, it has been shown by Matsubara and Toyozawa[3] that all these single-site terms can be summed up by renormalizing each point. The situation is illustrated by diagrams in Fig. 8. A small

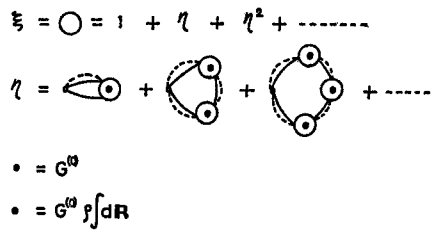

Fig. 8. Diagrammatic representation for the process of the self-consistent formulation.

open circle represents a site which is not summed, while a small filled circle designates a site over which the summation or equivalent integration is carried out. A large circle is used to indicate that an open or filled small circle inside the large circle is renormalized in the sense that an arbitrary number of rings are attached thereto. It is convenient to associate with a large circle a quantity ξ given by

$$\xi = 1+\eta+\eta^2+\cdots = \frac{1}{1-\eta}, \tag{4·1}$$

where the renormalization is effected by writing η as

$$\eta = [G^{(0)}]^2 \xi \rho \int H(\boldsymbol{R}_{12}) H(\boldsymbol{R}_{21}) g(\boldsymbol{R}_{12}) d\boldsymbol{R}_{12}$$

$$+[G^{(0)}]^3(\xi\rho)^2\int H(\boldsymbol{R}_{12})H(\boldsymbol{R}_{23})H(\boldsymbol{R}_{31})g(\boldsymbol{R}_{12})g(\boldsymbol{R}_{23})g(\boldsymbol{R}_{31})d\boldsymbol{R}_2d\boldsymbol{R}_3+\cdots$$

$$=[G^{(0)}]^2\xi\rho\int\frac{[V(\boldsymbol{k})]^2}{1-\xi\rho G^{(0)}V(\boldsymbol{k})}\frac{d\boldsymbol{k}}{(2\pi)^3}+[G^{(0)}]^2\xi\int\rho V(\boldsymbol{k})[V_0(\boldsymbol{k})-V(\boldsymbol{k})]\frac{d\boldsymbol{k}}{(2\pi)^3}. \tag{4·2}$$

It is easy to see that the diagonal element of the ensemble-averaged Green function is related to ξ by

$$\xi=E\langle G_{mm}(E)\rangle=w\cdot V_0\langle G_{mm}(w)\rangle, \tag{4·3}$$

and therefore the self-consistent solution of associated equations (4·1) and (4·2) yields the density-of-states via Eqs. (4·3) and (2·10). The numerical calculation of $n(E)$ along this line will be carried out in § 5 for various pair-distribution functions.

It is interesting to note that the self-consistent theory of the present paper is compared with the approximation by Schwartz and Ehrenreich.[4] In our theory, atomic correlations are considered such that diagram (a) in Fig. 9 is taken into account. On the other hand, in the approximation of Schwartz and Ehrenreich, those diagrams counted in our treatment are discarded but diagrams like (b) or (c) in Fig. 9 are included, where the formulation does not preserve the symmetry as to the atomic sites.

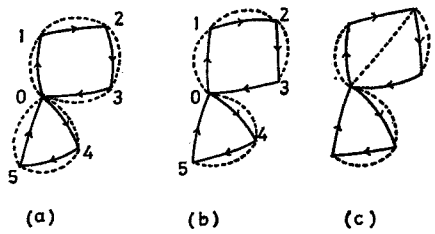

Fig. 9. Comparison between the self-consistent treatment in our theory (a) and that of Schwartz and Ehrenreich (b) or (c).

§ 5. Density-of-states in the self-consistent theory

In the present section, the density-of-states $n(E)$ is evaluated in the self-consistent framework using three model pair-correlation functions and one experimental data. Most of the calculations are performed for the concentration $p=0.2$, which corresponds to the atomic number density of a hard-core-random liquid satisfying $\eta=0.45$ and $\sigma=7.56$. Since the computer work[10] estimates the hard-core diameter of liquid transition metals to be about 2.2Å and the radius of $3d$ orbits in these metals are calculated to be approximately 0.3Å, the value $\sigma=7.56$ is considered to simulate some aspects of these metals.

5.1 *Random liquid*

The self-consistent density-of-states for a random liquid will be discussed in the following subsection as a limiting case of a hard-core-random liquid.

5.2 *Hard-core-random liquid*

The pair-distribution function defined by Eq. (3·7) is used to calculate the density-of-states. The results are illustrated in Figs. 10(a) and (b) in which p is fixed to be 0.2 and the packing fraction η is changed. Note that $\eta=0$ corresponds to a random liquid. According as η is increased, we notice the remarkable behaviour of (1) the band width and (2) the band shape.

As for (1), the larger η is, the narrower the band width becomes, and both the upper and lower edges move monotonically towards the centre of the band as shown in Fig. 11, where curves of the band edges vs. η are pictured and

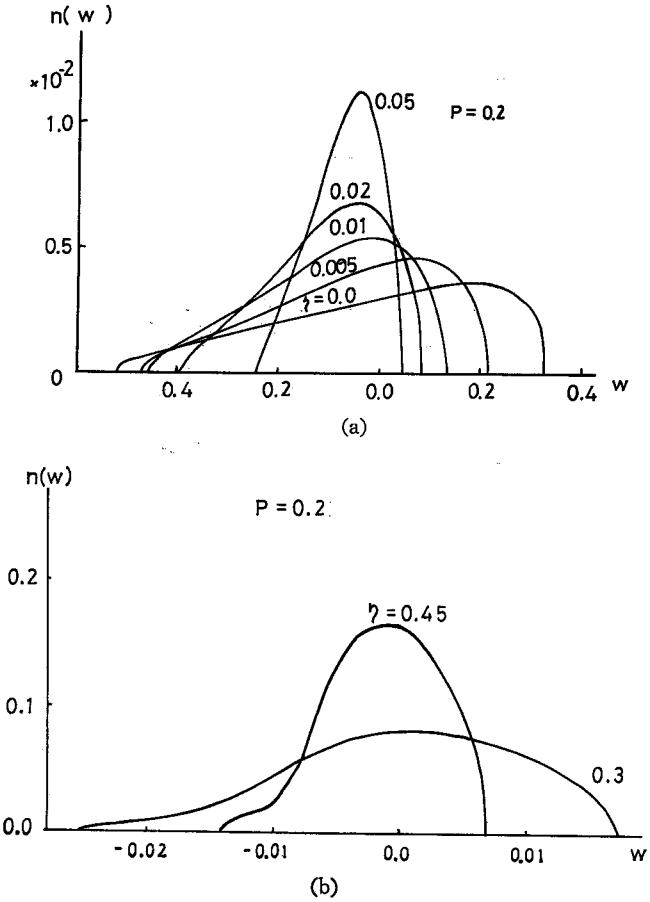

Fig. 10. The density-of-states for hard-core-random liquids for $p=0.2$. The parameters associated with the curves denote the packing fractions η. Thus, for (a), $\eta=0.0$, 0.005, 0.01, 0.02 and 0.05, and for (b), $\eta=0.3$ and 0.45 are employed.

compared with the edges due to the non-self-consistent calculation designated by dotted lines in the figure. The η-dependence of the upper band edge in the NSC theory is qualitatively different from that in the SC theory, and the latter is reasonable from physical point of view, while the former is not. Namely, the mentioned characteristics are attributed to the fact that the hard-core pair-correlation function of Eq. (3·7) cuts off the domain of integration at which the transfer matrix $H(R)$, related to Eq. (3·9) and expressed by Fig. 4, is most dominant. As a result, the effect of broadening the atomic level by means of the transfer integral is reduced and this reduction is more serious for a larger hard-core diameter. Note that $n(E)$ around the peak of the band increases as the band width decreases; it is ascertained that the accumulated density-of-states in a band is the same for all values of η and thus the sum rule is proved.

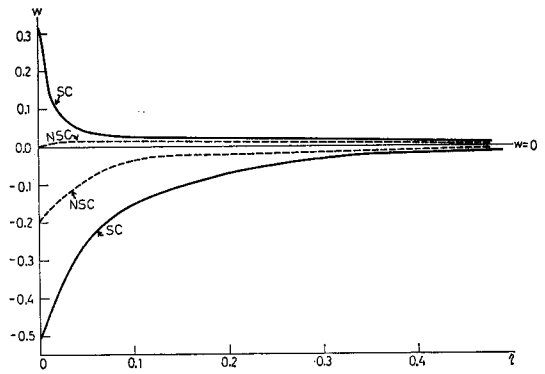

Fig. 11. Comparison of the band-edges due to the NSC calculation (dotted lines) and the SC calculation (solid lines).

Concerning (2), we can conclude from Figs. 10(a) and (b) that the band shape is most asymmetric for a random liquid with $\eta=0$ and a more and more symmetric density-of-states is obtained when the value η is increased. Here the term "symmetric" is used to express the symmetry of the band in the sense that the position of the peak is approximately at the centre of the band and the band tails at both the upper and lower edges are of the similar shape. In the first place, the reason for the asymmetry is explained as follows: Suppose we have a cluster made of N_0 atoms, in which the atomic levels for the constituent atoms are all identical, being equal to E_0, and the transfer integral between any two of atoms has also a common value $-V_t$. It is apparent that V_t depends on the size of the cluster. Eigenvalues for the energy of an electron in the cluster are obtained on solving the secular equation of N_0-th-order:

$$\begin{vmatrix} E_0-\lambda & -V_t & -V_t & \cdots & -V_t \\ -V_t & E_0-\lambda & -V_t & \cdots & -V_t \\ -V_t & -V_t & E_0-\lambda & \cdots & -V_t \\ \cdots & \cdots & \cdots & \cdots & \cdots \\ -V_t & -V_t & -V_t & \cdots & E_0-\lambda \end{vmatrix} = 0, \qquad (5\cdot1)$$

from which we have an (N_0-1)-fold degenerate eigenvalue $\lambda=E_0+V_t$ and a non-degenerate solution $\lambda=E_0-(N_0-1)V_t$. Therefore the bigger the number N_0 of atoms in the cluster is and the smaller the size of the cluster is, the more asym-

metric density-of-states is expected, and this explains the eminent feature of the band for small η. In the second place, approach to a symmetric shape for a large value of η is understood to be an outcome of hard-core pair-correlations which work to eliminate a large density fluctuation. In other words, the probability of finding clusters which are composed of many atoms brought together is decreased remarkably because of the geometric requirement for hard spheres. Consequently, a less random distribution of atoms is attained and the symmetric properties of the band for a regular system is recovered. This situation is also suggested from the consideration of Eq. (5·1) and the explanation thereabout. For the largest η calculated, i.e., $\eta=0.45$, the position of the peak is near the atomic level, $E_0=H_{nn}=0$, and the band is almost symmetric except for a small shoulder at the lower band edge. This shoulder is regarded as originating from the energy levels of clusters which happen to form in a partially ordered system and may serve as a sort of trap centres.

Figure 12 represents the calculated density-of-states in which η is taken to

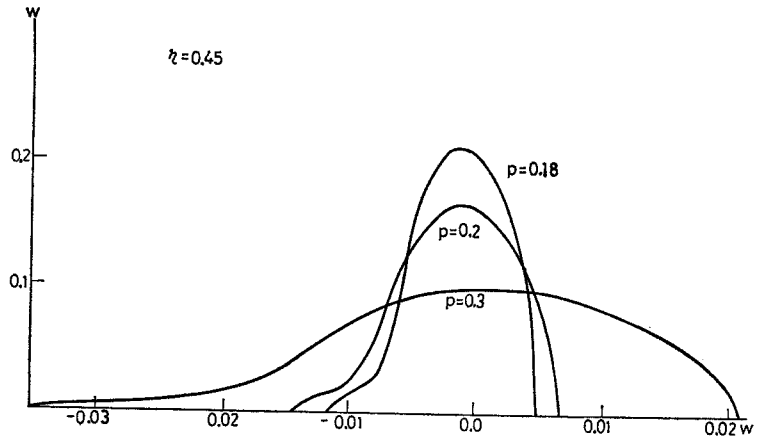

Fig. 12. The density-of-states for hard-core-random liquids. The packing parameter is fixed at 0.45 and the concentration p is changed.

be a fixed value 0.45 and the concentration p is changed. The constant packing fraction indicates that the corresponding systems are geometrically analogous and thus the degrees of randomness in these systems are not different. This predicts that, for various concentrations p, we may have the same symmetry of the band that is related to the degree of randomness. On the other hand, the increase of p under a constant η leads to the decrease of σ, the ratio of the hard-core diameter to the effective Bohr radius, as is seen from Eq. (3·8). The effect of bringing σ smaller is to include into the integrant the most dominant part of the transfer energy $H(R)$ and therefore to broaden the band. It is directly concluded from Fig. 12 that the increase of p gives rise to a wider band but does not alter the symmetry of the band shape. These results of the numerical cal-

culation coincide with the above-described theoretical conjecture.

It should also be noted that the difficulty of divergence encountered in the NSC calculation is now removed.

5. 3 *Hard-core-modified liquid*

In order to make the model pair-distribution function $g(R)$ more realistic, let us introduce a modified hard-core correlation defined by

$$g(R)=\begin{cases}0, & R/a^*\leq\sigma,\\ h, & \sigma<R/a^*\leq\sigma+\delta,\\ 1, & \sigma+\delta<R/a^*,\end{cases} \qquad (5\cdot2)$$

where $h\geq1$. The width δ of the modified part is determined so as to satisfy the given number z of the nearest-neighbour atoms by the following relation:

$$z=\rho\int_{\sigma a^*}^{(\sigma+\delta)a^*} g(R)\,4\pi R^2dR=\frac{4\pi\rho a^{*3}}{3}h[(\sigma+\delta)^3-\sigma^3]. \qquad (5\cdot3)$$

In Fig. 13, the density-of-states for a hard-core-modified liquid is shown by the curve (b) in comparison with the curve (a) of the hard-core-random liquid. For numerical calculation, h is chosen to be 2. Three distinguished features are recognized:

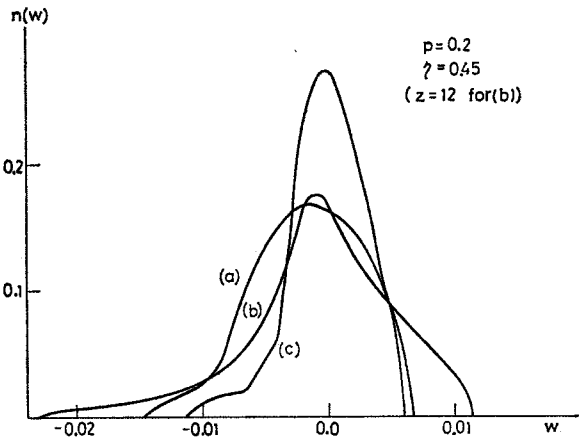

Fig. 13. Comparison of the calculated density-of-states for (a) a hard-core-random liquid, (b) a modified hard-core liquid and (c) a real liquid. The packing fraction η is 0.45 for all the three cases. For a hard-core-modified liquid of (b), the coordination number z is taken to be 12.

(1) The band of (b) is broader than that of (a). This is due to the fact that the elevated portion in $g(R)$ for $\sigma\leq R/a^*\leq\sigma+\delta$ works to emphasize the contribution from the dominant part of the transfer matrix $H(R)$; thus a wider band being expected.

(2) A hard-core-modified liquid has a steep denstiy-of-states around the atomic level compared with $n(E)$ for a hard-core-random liquid. This is explained as follows: The probability of finding atoms within the shell ($\sigma\leq R/a^*\leq\sigma+\delta$) is greater than that of having atoms outside the shell, which yields a more regular system as a whole, and thus some properties of a regular system appear.

(3) The band tail at the lower edge is remarkable. The same reason as in (2) for having larger probability density in the shell causes a local fluctuation, since the formation of clusters with a larger number of atoms is promoted. This pro-

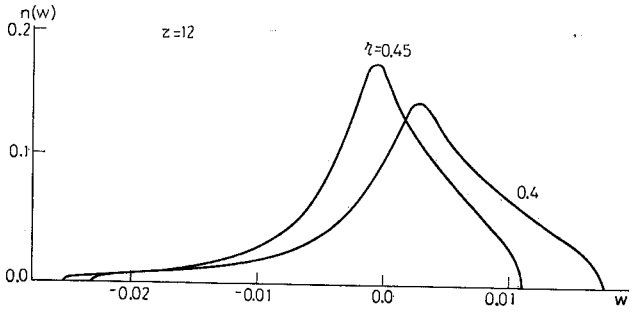

Fig. 14(a). The density-of-states for two hard-core-modified liquids with $z=12$, $p=0.2$ and η is changed ($\eta=0.4$ and 0.45).

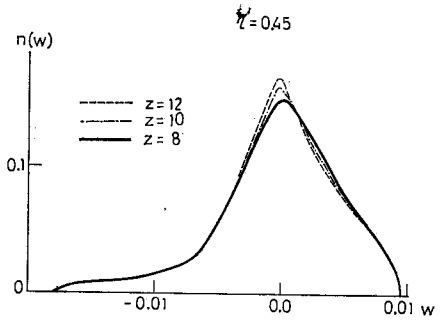

Fig. 14(b). The density-of-states for three hard-core-modified liquids with $z=12$, 10 and 8.

vides energy levels somewhat deep in the tail of the lower band edge.

Figure 14(a) represents the η-dependence of the density-of-states of hard-core-modified liquids with $z=12$ and $p=0.2$. The tendency that a larger packing fraction gives a narrower and more symmetric band is here again observed.

In Fig. 14(b), three different hard-core-modified liquids are compared, where the packing fraction $\eta=0.45$ and the concentration $p=0.2$ are fixed and only the coordination number z is changed. Comments are made on two points.

(1) As the hard-core diameter remains constant for these three cases, the cutoff of the integration domain takes place at the same distance $R=\sigma a^*$ and therefore the contribution from the dominant transfer matrices is also unchanged. This is the reason why the shape of the band in the both tail regions is not altered for different values of z.

(2) When z is increased under the condition that σ is constant, only the width δ of the first peak in $g(R)$ becomes large. However, the change of δ is not so serious as that of z as is apparent from Eq. (5·3). Moreover, the effect of the transfer matrix around $R=(\sigma+\delta)a^*$ is to broaden the atomic level approximately as much as $H((\sigma+\delta)a^*)$, which is rather small for parameters under consideration. This accounts for the numerical results in Fig. 14 that the sharpness of the peak near the atomic level is slightly modified when z shifts from 8 to 12.

From the above two remarks, we can conclude that the shape of the band in the tail regions is determined from the hard-core diameter or from the behaviour of $g(R)$ around the core-cutoff, while the sharpness, height, etc., of the density-of-states peak is determined from the nature of the first peak in $g(R)$.

5.4 *Real liquid*

Finally, we apply our theory, for illustration, to the pair-distribution function for a real liquid. The observed structure factor $a(k)$ for Ni at $T=1500°C$[11] is compared with the exact solution of the Percus-Yevick equation for a hard-sphere

liquid[12] and, for given values of p and σ moderately chosen from the physical consideration, the packing fraction is determined such that the first peak in $a(\boldsymbol{k})$ of the experimental result agrees with the calculated $a(\boldsymbol{k})$ of the Percus-Yevick hard-core liquid. The density-of-states, which is calculated using the radial distribution function $g(R)$ obtained from $a(\boldsymbol{k})$ for Ni, is shown by curve (c) in Fig. 13, in comparison with the results of a hard-core-random liquid (curve(a)) and of a hard-core-modified liquid (curve(b)). Since the characteristic feature of $g(R)$ for a real liquid guarantees the configuration more regular than that of the model liquids adopted in this article, the sharper and higher peak around the atomic level is attained. On the other hand, the real pair-correlation function indicates a less probability of finding atoms just outside the "so-called" hard sphere in contrast to the model distributions and this is understood to be the origin of a narrower band for a real liquid.

§ 6. Some remarks on the localization of electrons and conductivity

Let us consider in the present section the problem of electron localization

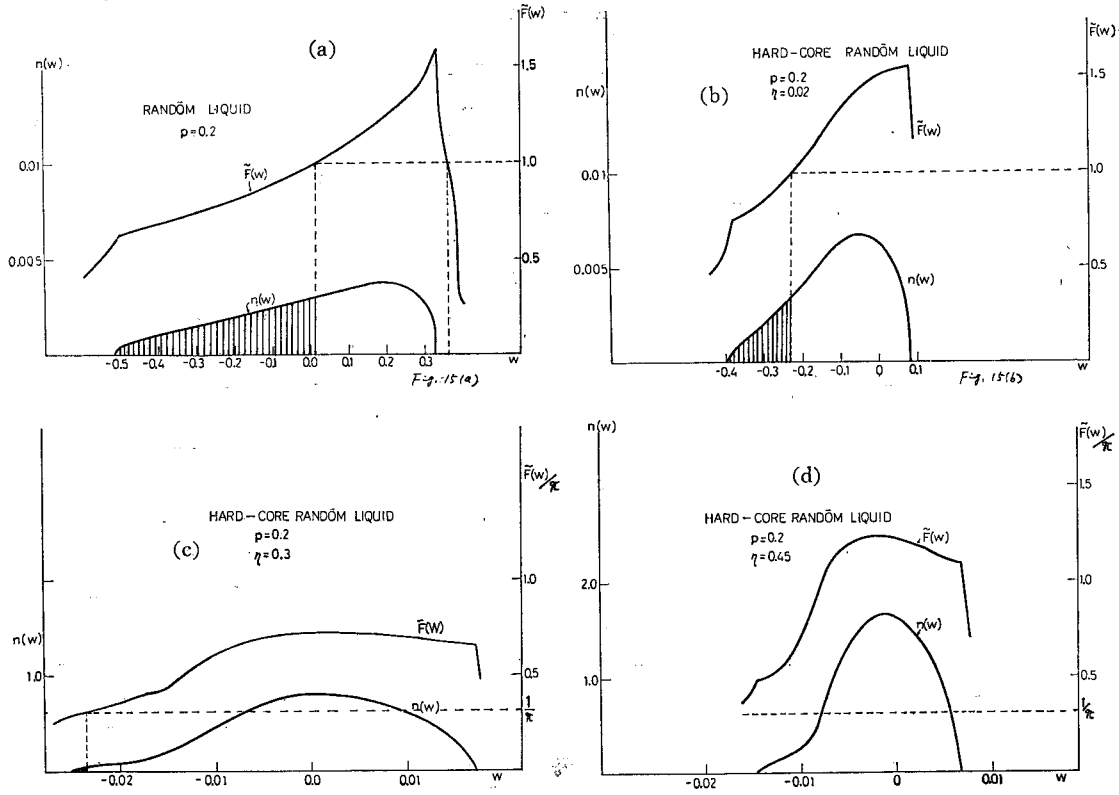

Fig. 15. Modified localization function $\tilde{F}(w)$ vs. w curve compared with the density-of-states $n(w)$. Numerical calculations are performed for several values of η; i.e., (a) $\eta=0.0$, (b) $\eta=0.02$, (c) $\eta=0.3$ and (d) $\eta=0.45$. The concentration $p=0.2$ for all figures.

in the calculated band for structurally disordered systems such as liquids, amorphous solids and doped semiconductors. For systems with cellular disorder, Economou and Cohen[13] introduced a localization function $F(E)=E_b/|E-\Sigma(E)|$ to check the localizability of electronic states corresponding to eigenenergy E. The $\boldsymbol{k}$-independent self-energy $\Sigma(E)$ is defined by an ensemble-averaged one-electron Green function by the relation $G_k(E)=[E-E_k-\Sigma]^{-1}$ and E_b denotes the half-width of the band for the corresponding regular system. They argue that the state with energy E is localized if $F(E)<1$. Although the localization function given by them cannot be directly applied to our problem where structurally disordered systems are treated, it would be reasonable to extend the definition of the localization function by replacing E_b by a quantity which serves as a measure for the half-width of our density-of-states and thereafter to make use of the modified localization function for the purpose of estimating the degree of localization in systems with structural disorder. The modified localization function may be written as

$$\tilde{F}(E)=\frac{\rho\int H(\boldsymbol{R})g(\boldsymbol{R})d\boldsymbol{R}}{|E-\Sigma(E)|}. \tag{6·1}$$

A smaller value of $\tilde{F}(E)$ is considered to correspond to a more localized state. In Fig. 15, $\tilde{F}(w)$ $(w=E/V_0)$ for several values of η are plotted. For small values of η (curve (a) with $\eta=0.0$ and curve (b) with $\eta=0.02$), the asymmetric property of the density-of-states is reflected to the behaviour of $\tilde{F}(w)$ and the states near the upper band edge are extended, while the states in the lower band tail are localized. This result seems to be reasonable from physical point of view. According as the symmetric property of the band is recovered accompanying the increase of η (curve (c) with $\eta=0.3$ and curve (d) with $\eta=0.45$), the asymmetric feature of $\tilde{F}(w)$ slips off and the states in the middle of the band become more extended. The absolute value of $\tilde{F}(w)$ increases when the packing fraction is made large, and this is consistent with our conjecture that a less random configuration is obtained for a greater value of η. Note that $\tilde{F}(w)$ in Figs. 15(c) and (d) are scaled by π. If the criterion $F(w)<1$ is employed to test the localization of electrons, we can see that, for $\eta=0.0$, about two thirds of low-energy side in the band are localized, while only the states lower than the middle of the band are localized for $\eta=0.02$. The energy region in which the states are localized decreases monotonically when the packing fraction is made bigger. For η as large as 0.3, only the small region in the lower band tail corresponds to localized states, while for $\eta=0.45$ almost all states are extended.

In Fig. 16, the electrical conductivity σ and mobility μ are plotted as a function of the Fermi energy $w=w_F$ and compared with $\tilde{F}(w)$. The conductivity $\sigma(w)$ is evaluated on the basis of the Kubo-Greenwood formula and the ensemble average of two Green functions $\langle G_{\boldsymbol{k}\boldsymbol{k}'}(E)G_{\boldsymbol{k}'\boldsymbol{k}}(E')\rangle$ is approximated by the product $\langle G_{\boldsymbol{k}\boldsymbol{k}'}(E)\rangle\langle G_{\boldsymbol{k}'\boldsymbol{k}}(E')\rangle$. The mobility at the Fermi level is determined

by $\mu(w_F) \propto \sigma(w_F)/n(w_F)$. The w_F-dependence of mobility expressed by a dotted line in the figure indicates that the mobility is large in the lower band tail and rather small for higher energy. This result is inconsistent with the behaviour of $\tilde{F}(w)$ and is not compatible, as well, with the widely-accepted knowledge that the states in the lower band tail are generally localized. This inappropriate suggestion of the calculated mobility is considered to come from the crude approximation $\langle GG \rangle \simeq \langle G \rangle \langle G \rangle$.

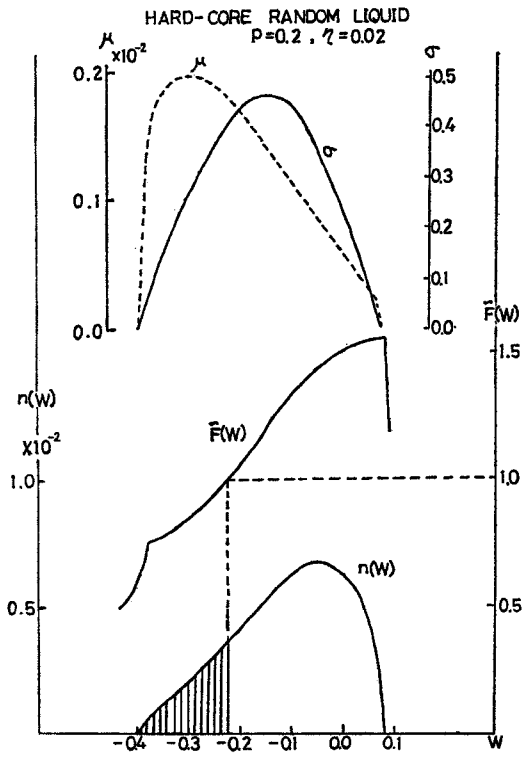

Fig. 16. Electrical conductivity σ and mobility μ as functions of the Fermi energy $w=w_F$; $\tilde{F}(w)$ and $n(w)$ are also plotted for comparison.

§ 7. Discussion

In the present paper, we have proposed a method to study the electronic structure of topologically disordered systems in which a short-range order in the atomic distribution is retained, while a long-range order characteristic of the crystal is lost. The one-electron Green function $G(w)$ is expanded in the tight-binding representation and a partial summation of the perturbation expansion series for $G(w)$ is derived. In the summation, the effect of clustering is included by counting all sorts of complicated single-site diagrams up to the infinite order. The atomic distribution functions are expressed by means of pair-correlation functions $g(R)$ based upon the extended chain approximation and taken into account in the process of ensemble-average. For actual calculation, some of model liquids and one real liquid are employed, and the radial distribution functions for these liquids are made use of. The density-of-states, etc., are evaluated in accordance with the non-self-consistent (NSC) scheme and the self-consistent (SC) scheme in our theory. It has been concluded that making the treatment self-consistent is essential in several respects. Especially, singularities inherent in the NSC calculation of the density-of-states are removed when the SC theory is applied. Moreover, the SC theory gives a physically reasonable dependence of the band-

edge position on the packing fraction, while the NSC theory fails to. Another conclusion is that, even in the framework of the extended chain approximation for the atomic configuration and the single-site treatment of the perturbation series of $G(w)$, the calculated density-of-states and other electronic properties reflect the short-range order which is measurable in terms of the atomic distribution functions. Although some quantitative alternation may be introduced when the approximations are improved, it is expected that the qualitative features of the density-of-states reflecting the types of pair-correlation functions are substantially unmodified.

Several possibilities are considered in order to develop better approximations. One possible step is to include higher-order terms such as double-site diagrams as shown in Fig. 17. The transfer integral $H(\boldsymbol{R})$ multiplied by $g(\boldsymbol{R})$ in the above formulation may be replaced by $H(\boldsymbol{R})g(\boldsymbol{R})[1-\{G^{(0)}\}^2H(\boldsymbol{R})H(-\boldsymbol{R})]^{-1}$. Another way to improve the approximations is to relax the condition of a quasi-orthogonal set of atomic orbitals and to count the effect of non-orthogonality, which will be studied in a succeeding paper.[7]

Fig. 17. Some of the double-site diagrams.

Although most of the discussion and numerical calculations are concerned with some models for liquid metals, the theory is as well applicable to amorphous metals, doped semiconductors, etc. In the popular doped semicondutors of physical interest, the hard-core diameter σa^* is comparable with the ion-core diameter and is of about a few Å, while the effective Bohr radius is far larger, i.e., $\sim$100Å, and therefore σ is small, which corresponds to a small packing fraction η.

Acknowledgements

The authors are deeply indebted to Prof. M. Watabe for fruitful discussions and a critical reading of the manuscript. They are also obliged to Prof. M. Hori for stimulating conversations and grateful to Dr. M. Nakamura for valuable advice in the numerical calculations.

References

1) F. Cyrot-Lackmann, Adv. Phys. **16** (1967), 393.
2) L. H. Roth, Phys. Rev. Letters **28** (1972), 1570.
3) T. Matsubara and Y. Toyozawa, Prog. Theor. Phys. **26** (1961), 739.
4) L. Schwartz and H. Ehrenreich, Ann. of Phys. **64** (1971), 100.
5) M. Lax, Phys. Rev. **85** (1952), 621.
6) R. C. Chaney, C. C. Lin and E. E. Lafon, Phys. Rev. **B3** (1971), 459.
7) F. Yonezawa and Y. Ishida, "Electronic Structure of Liquid Metals in the Tight-Binding

Approximation. II—*Nonorthogonal Set of Atomic Orbitals*—", to be submitted to Prog. Theor. Phys.

8) H. Renkert, F. Hensel and E. U. Franck, Phys. Letters **31A** (1969), 494.
Ber. Bunsenges, Physik. Chem. **75** (1971), 507.
V. A. Alekseev, ZETF **14** (1971), 295.

9) F. Yonezawa, M. Watabe, M. Nakamura, Y. Ishida and T. Ogawa, *Proceedings of the Second International Conference on "The Properties of Liquid Metals"*, held in Tokyo (September, 1972).
F. Yonezawa, M. Watabe, M. Nakamura and Y. Ishida, "Electron Correlations and the Metal-Nonmetal Transition in Structurally-Disordered Systems—*General Theory and Application to Supercritical Alkali Metals*—", submitted to Phys. Rev. (1973).

10) D. Schiff, Phys. Rev. **186** (1969), 151.

11) Y. Waseda, K. Suzuki, S. Tamaki and S. Takeuchi, Phys. Stat. Sol. **39** (1970), 181.

12) N. W. Ashcroft and J. Lekner, Phys. Rev. **145** (1966), 83.

13) E. N. Economou and M. H. Cohen, Phys. Rev. **5** (1972), 2931.